

Characteristics-Based Design of Multi-Exponent Bandpass Filters

Samiya A Alkhairy

Abstract—We develop methods to design bandpass filters given desired characteristics such as peak frequency, bandwidth, and group delay. We develop this filter design method for filters we refer to as Generalized Auditory Filters (GAFs) which are represented as second order filters raised to non-unitary exponents and hence have three degrees of freedom. Our method for filter design accommodates specification of a trio of frequency-domain characteristics from amongst the peak frequency, convexity, 3dB, ndB quality factor, equivalent rectangular bandwidth, maximum group delay, and phase accumulation. To develop our characteristics-based design methods, we derive expressions for the filter constants directly in terms of filter characteristics. The parameterization of GAFs in terms of sets of characteristics allows for specifying magnitude-based characteristics (e.g. bandwidths) and phase-based characteristics (e.g. group delays) simultaneously. This enables designing sharply tuned filters without significant group delay, and is particularly important in filterbanks where frequency selectivity and synchronization are both important aspects of design. Using our methods, we directly dictate values for desired filter characteristics - unlike iterative filter design methods. This allows for more direct design of GAFs for phase-picking from seismic signals, cochlear implants, and rainbow sensors. The methods also directly apply to related bandpass and multi-band filters.

Index Terms—Filter design, quality factor, group delay, tunable filters, IIR filters, bandpass filters, multi-band filters, auditory filterbanks.

I. INTRODUCTION

A. Existing Methods for Filter Design

Existing filter design paradigms for digital filters generally aim to estimate filter coefficients that meet certain criteria - e.g. maximally flat response in the passband, equiripples, specified cut-off frequencies, frequency response. The filter design problem is formulated to be optimal in some chosen sense [1]. Filter design methods are generally developed in the frequency domain, but may also be in the time domain [2]. There are several methods for digital filter design, which may generally be categorized as (1) iterative optimization-based design (for both FIR and IIR filter design) [3], and (2) direct design based on analog prototype filters (for IIR filter design).

Digital filter design of IIR filters is classically done based on analog prototype filters - such as Butterworth and Chebyshev, that are stable and have known optimal behavior (e.g. optimal conditions on ripples in the pass/stopband and flatness) and then converted to a digital filter using techniques such as bilinear transforms. In addition to the analog-prototype-based method for designing IIR filters, there also exist optimization-based methods for solving for IIR filter coefficients. Several

iterative methods originally developed for FIR filters have been extended to formulate and solve optimization-based filter design methods for IIR filters - though the problem is more involved due to issues of stability and pole-zero placement. FIR filter design is generally carried out by solving an optimization problem to find coefficients to minimize some cost function on the difference between the target and actual frequency response specification. A filter form and order are specified, and a desired specification of a set length is supplied. This specification may be on magnitude, amplitude [4], or the entire frequency response [5]. The objective function is defined based on certain criteria on - e.g. minimax and least squares [1], then solved for coefficients.

Solvers for the least square formulation allow for easily dealing with the complex frequency response but are generally not desirable except in the special case where the problem is linear in coefficients. The minimax problem is classically solved using Parks-McClellan algorithm (a Remez exchange algorithm for filters) which limits the minimax formulation to real problems. This translates into only using specifications on the amplitude rather than than the full complex frequency response. This is feasible for linear-phase FIR filter design where we can neglect the phase and limit ourselves to a real alternative - the amplitude of the frequency response. There are also extensions of exchange algorithms that go beyond the limitations of the Parks-McClellan algorithm and allow for: using the minimax formulation for the entire (complex) frequency response for FIR filters thereby allowing for handling arbitrary phase as well [5]; formulating and solving minimax problems for designing stable IIR filters with magnitude specifications [6]; and designing sparse - and hence computationally efficient, linear-phase FIR filters [7]. More recent filter design methods include seeker-optimization algorithms [8], differential evolution algorithms [9], gravitational search algorithms [10], and deep-learning methods [11].

B. Proposed Method for Bandpass Filter Design

Our filter design method, developed here for certain classes of bandpass filters, does not fall into either category of classical filter design methods mentioned in the previous section - (1) iterative optimization based methods, and (2) direct design based on analog prototype filters. Instead, our method designs filters based on desired sets of frequency domain characteristics - such as peak frequency, quality factors, and group delay at the peak frequency. This (3) characteristic-based method for filter design may be considered a distinct category. The method: (a) is direct, non-iterative, and computationally efficient, (b) requires a small number of desired

S. Alkhairy is with MIT, Cambridge, MA, 02139, USA. e-mail: samiya@mit.edu

filter characteristics rather than an entire frequency response, and (c) can naturally be formulated based on phase and/or magnitude based filter characteristics to fulfill requirements on delay, selectivity and synchronization in filterbanks, and/or fine control over the shape of the filter. In developing our characteristics-based filter design method, we are motivated by second order bandpass filters which describe a variety of systems.

1) *Motivation for Characteristics-Based Filter Design:*

One particularly important, and unique, feature of second order bandpass filters is the ability to design them based on desired frequency domain filter characteristics due to their parameterization in resonant frequency and quality factor - this is in contrast to iterative filter design methods that attempt to estimate filter coefficients based on a given desired frequency response and specifications.

To give a concrete example of filter design using filter characteristics, consider the example of a lightly-damped driven harmonic oscillator (in its region of operation as a bandpass filter) which may be parameterized using the approximate 3-dB quality factor and peak frequency as,

$$H(s) = \frac{1}{s^2 + \frac{\omega_n}{Q_3}s + \omega_n^2}. \quad (1)$$

This parameterization enables designing filters for second order systems using desired filter characteristics Ψ - the 3-dB quality factor, Q_3 , and the peak frequency of the undamped system, ω_n .

We may consider a representation of the second order system that only has a single degree of freedom - Q_3 , if we consider the equivalent expression where s is defined based on normalized angular frequency, $\frac{\omega}{\omega_n}$ rather than on ω ,

$$H(s) = \frac{1}{s^2 + \frac{1}{Q_3}s + 1}. \quad (2)$$

Currently, such characteristics-based filter design is limited to second order bandpass filters and other particularly simple filters. However, as second order systems only have a single degree of freedom other than the resonant frequency, their behavior is limited. For instance, the phase accumulation is fixed to half a cycle, the ratio of bandwidth to group delay is fixed, as is the ratio of sets of two bandwidths of different levels (e.g. 3dB BW to 15 dB BW). On the other hand, when using other filters with wider ranges of behavior to process signals, we lose the ability to design those filters based on desired filter characteristics.

2) *Goal:* Here, we develop methods for characteristic-based design of filters with two degrees of freedom other than the peak frequency. These filters may be considered a cascade of second order filters where all constitutive filters have the same peak frequency, thereby resulting in a bandpass filter with a single clear peak rather than one with a flat magnitude response in the bandpass region.

In this paper, we introduce a characteristics-based method for filter design for a class of bandpass filters that represents processing in various systems and is of the form,

$$H(s) = C((s-p)(s-\bar{p}))^{-B_u}, \quad (3)$$

where $-\text{Re}\{p\}, \text{Im}\{p\} \in \mathbb{R}^+$ and $B_u \in \mathbb{Z}^+$ resulting in an all-poles filter with a single repeated pair of complex conjugate poles in the left half plane¹. We refer to these filters in the bandpass region of operation as Generalized Auditory Filters (GAFs). In the case of filterbanks, our characteristic-based filter design method is particularly valuable due to frequency separation and synchronization requirements between the various filters in the filterbank.

3) *Filter Design Method:* The bandpass filter design presented in this paper results in the ability to design the filters by specifying values for viable sets of three frequency domain filter characteristics, Ψ . These filter characteristics may include: peak frequency, 3 dB bandwidth, 10 dB bandwidth, equivalent rectangular bandwidth, phase accumulation (the difference between maximum and minimum phase), group delay at the peak frequency, as well as convexity (the second derivative of the magnitude at the peak) - a characteristic we introduce in this paper which is a peak-centric measure of sharpness of tuning. Consequently, we only require three values - for the three chosen filter characteristics, to design the filter. This is in contrast to classical filter design methods of the first category which are iterative and also require the frequency response (or its magnitude or amplitude) over some length of frequencies.

4) *Approach for Developing Filter Design Method:* In developing our methods for characteristics-based parameterization and design for such filters, it is not possible to simply extrapolate and use the equations for characteristics of the related second order systems (or equivalently, place poles based on the quality factor of the associated second-order system). Instead, the characteristic-based parameterization must be properly derived from the expressions for the higher order filter itself.

Our filter design paradigm collapses the problem into one of expressing filter constants, Θ - the pole and filter exponent (or alternatively, filter coefficients), in terms of desired filter characteristics, Ψ , such as peak frequency, quality factor, phase accumulation, and maximum group delay. Using our derived expressions for filter constants in terms of characteristics, we may parameterize the GAFs using a subset of these filter characteristics. In this paper, we denote filters for which we may apply these direct characteristic-based filter design methods as ‘tunable’ filters (in the narrow sense that we have explicit control over the characteristics and can directly tune the filter to match the desired values for characteristics without the need for iteration) or ‘parametizable’ filters (in the narrow sense that the filters can be parameterized by filter characteristics instead of generic constants).

5) *Related Filters:* As most of the filter characteristics we consider for filter design in this paper are peak-centric, our methods also approximately apply to filters that are related to GAFs - e.g.,

$$H(s) = C s^c ((s-p)(s-\bar{p}))^{-B_u}, \quad \text{with } c < B_u. \quad (4)$$

¹The constant B_u , is in fact not limited to positive integer values and may take on positive rational values. However, the stability, causality, and reliability of the non-integer exponent case is not discussed here and we instead address it in separate work [12]

We can design such filters based on the characteristics-based parameterization derived in this paper for GAFs provided that the zero is far enough from the peak frequency. Additionally, the characteristics-based design paradigm presented here for single-band filters can be used for dual-band and multi-band filters with distinct peaks. Consequently, the filter design approach developed here can be used for a wider variety of filters than GAFs (equation 3) - which itself may be used for a wide range of applications.

6) *Applications of Chosen Filters, Filterbanks, and Multi-band Filters:* Filters that can be represented using equation 3 and related representations occur in a wide variety of systems, the most trivial of which are second order systems - such as RLC circuits, which have been studied extensively. Filterbanks composed of such filters and similar ones (e.g. gammatone filters) are also useful for phase-picking from micro-seismic recordings [13], spike-based pattern recognition and seismic event detection [14], industrial fault diagnostics - including those used in nondestructive testing [15], rainbow sensors [16], underwater sound classification and target feature extraction [17], cochlear implants [18], [19], [20], speech feature extraction and speech recognition [21], noise reduction and control [22], environmental sound classification [23], bird sound classification [24], speech-based diagnostics [25], signal processing in heart-abnormality diagnostics [26], lung pathology diagnostics [27], vocal pathology classification [28], bio-mimetic sonar [29], perceptual studies, compressing audio files, and potentially hearing aids [30], [31]. Associated multi-band filters may also be used for a wide range of applications such as auditory equalizers [32] and signal processing for denoising signals from mechanical systems with known properties [33]. Proper filter design will enable maximizing information obtained from each of these processed signals. The ability to parameterize the filters to directly control their behavior (as is the case with the characteristic-based filter design paradigm proposed here) would allow us to better - and more directly, tune filters for their intended applications.

C. Objectives and Scope

In this paper, we present a characteristics-based filter design paradigm for a class of bandpass filters represented by equation 3, and for related bandpass filters. In section II, we introduce these filters in more detail in section. In section III, we develop the filter design paradigm which results in filters that can be parameterized by various sets of frequency domain filter characteristics, Ψ . These characteristics may include peak-centric characteristics such as peak frequency, quality factor, and group delay at the peak frequency. They do not include measures of asymmetry of the transfer function. The resulting tunability is especially important for filterbanks. The filter design paradigm introduced here allows us to directly dictate desired values for Ψ without iteration. This is as opposed to a typical approach of essentially iterating over the following steps: specifying values for filter constants, Θ , and generating the associated transfer function, then computing the characteristics and determining the error between desired and computed filter characteristics, then adjusting the filter constants.

Even though the filters in equation 3 are not restricted to those relevant for processing sounds, we have referred to them as Generalized Auditory Filters/Filterbanks (GAFs). For certain ranges of values of the filter constants and their variation within a filterbank, the GAFs mimic auditory/cochlear signal processing at low sound levels [34] and will be referred to as Auditory Filters / Filterbanks (AFs). For several of the diverse applications mentioned above, performance is desirable when the filters mimic cochlear signal processing and behavior (e.g. the ratio of quality factor to group delay). Indeed, certain multiplexing filter topologies are even inspired by the cochlea [35].

We demonstrate the accuracy of our characteristics-based filter design approach using AFs and second order systems in sections III-E and III-F respectively. This fulfills testing needs for two realizations of GAFs: those with ranges of filter constant values for AFs, and those for second order systems in which $B_u = 1$. Finally, we discuss using the proposed filter design method for associated multi-band filters.

II. FILTER EXPRESSIONS

In order to develop our characteristic-based filter / filterbank design method, we first introduce the GAF expressions in more detail. Instead of considering filters in angular frequency, ω , we consider them in terms of,

$$\beta \triangleq \frac{\omega}{\omega_{peak}}, \quad (5)$$

similar to equation 2. As we express the filters in terms of normalized (angular) frequency, β , rather than angular frequency, ω , the filter characteristics are defined in β (in section III). However, they can simply be redefined for filters in ω , by replacing β with ω .

We use normalized frequency, β , for two reasons: (1) In the case of filterbanks constituted of constant-Q filters (which all have the same quality factors but different peak frequencies and bandwidths), the filter representation in terms of β requires the same set of filter constant values across all filters; and (2) AFs (GAFs that mimic auditory signal processing in the cochlea) can be associated with certain cochlear models in which the peak frequency and bandwidths vary along the cochlear length (vary with filters in the auditory filterbank) in such a way, that locally, the filters can be considered a function of β (or locally, constant-Q).

In the particular case of filterbanks (in parallel configurations), we must set the peak frequency of each constitutive filter based on some predetermined designed variation within the filterbank. For instance, for auditory filterbanks, it is desirable to have the peak frequency for the constitutive filters follow the variation of peak frequencies along the length of the cochlea. In this case, we may express β as,

$$\beta = \frac{f}{CF(x)}, \quad (6)$$

where $CF(x)$ is the characteristic frequency map which takes the form, $CF(x) = CF(0)e^{-\frac{x}{v}}$. This mapping is quite useful for designing AFs in a parallel filterbank configuration in which each constitutive filter mimics cochlear signal

processing until a point x along the length of the cochlea. However, this assumed variation is generally not required for GAFs.

In constructing the filter expressions for GAFs, we use notation from AFs introduced in [34] which derives expressions based on a mechanistic model of the cochlea. The model not only contains variables for filters but also mechanistic variables that we are not concerned with in this paper. We note that the parameterization of filter variables based on filter characteristics is also useful for the scientific study of how the cochlea works and not just for signal processing applications that use AFs. However, in this paper, we are solely interested in the filter variables and not the mechanistic variables, and hence we refer to the filter and model interchangeably. Other formulations of the auditory filter that share similarities with our expressions include APGF and OZGF for which various implementational architectures have been developed [36].

As a result of using β , we redefine s , when purely imaginary to be,

$$s(\beta) = i\beta. \quad (7)$$

The GAFs² are represented as,

$$\frac{P(x, \omega)}{v_{st}(\omega)} = C \left((s-p)(s-\bar{p}) \right)^{-B_u} \quad (8)$$

where $p = ib_p - A_p$ and $\bar{p} = -ib_p - A_p$, and the outputs of the filterbank being $P(x, \omega)$ for an input, $v_{st}(\omega)$. The model constants A_p, B_u, b_p take on real positive values, and for the case of AFs they vary slowly along the length of the cochlea (allowing us to approximate it locally as constant-Q) [34].

As specifying the gain constant is trivial, we consider the GAF variable to be $\mathbf{P}(\beta)$,

$$\mathbf{P}(\beta(x, \omega)) \triangleq \frac{P(x, \omega)}{C v_{st}(\omega)} = \left((s-p)(s-\bar{p}) \right)^{-B_u} \quad (9)$$

to develop our filter design paradigm. \mathbf{P} at a particular location (a particular filter within the filterbank) is a transfer function in the form of equation 3.

Clearly, for the case of the exponent, B_u , being a positive integer, equation 9 represents rational transfer functions that are stable and causal IIR filters. Indeed, for the case of $B_u = 1$, the GAFs represent second order systems that describe classical physically-realizable systems.

A second, related, filter variable - which we may refer to as V , may be obtained from 9 by increasing the filter exponent from B_u to $B_u + 1$ and introducing a zero at $-A_p$ ³. This filter behaves most similarly to P when the filter is sharply tuned. Peak-centric filter characteristics are expected to be similar for both types of filters for reasonable values of A_p .

The magnitude (in dB) and phase of \mathbf{P} may be easily obtained from the real and imaginary parts of $\log(\mathbf{P})$ which we use in developing our filter design paradigm in section III. One

²In the cochlear model corresponding to AFs, the filter/response variable P corresponds to differential pressure right across the organ of Corti (OoC), $P(x, \omega)$, and the input, $v_{st}(\omega)$, is the stapes velocity

³This is related to V of the cochlear model - the velocity of the Organ of Corti partition

final variable we define in this section to aid in developing our filter design method is $k_\beta(\beta)$ ⁴,

$$k_\beta(\beta) = i \frac{d \log(P)}{d\beta}. \quad (10)$$

The expression for $k_\beta(\beta)$ associated with equation 8 is,

$$k_\beta(\beta) = 2B_u \frac{s + A_p}{(s-p)(s-\bar{p})} = B_u \left(\frac{1}{s-p} + \frac{1}{s-\bar{p}} \right), \quad (11)$$

where we have included the partial fraction decomposition which greatly simplifies our derivation in the following sections.

III. FILTER DESIGN AND MODEL TUNABILITY

In this section, we develop the characteristic-based filter design method (filter tunability) which will enable us to generate GAFs with desired frequency domain filter characteristics. The filter expressions in the previous section are parameterized by the pole and filter order, or alternatively, by the model constants $\Theta = [A_p, b_p, B_u]$. We aim to instead parameterize the GAFs in terms of reported or desired frequency-domain filter characteristics, Ψ , which describe the behavior of the magnitude and phase of the transfer functions. These filter characteristics include bandwidths, quality factors, maximum group delays, peak frequencies, phase accumulations. In this paper, we are not concerned with the associated time-domain characteristics - whether those based on step responses or impulse responses [37], as those require separate derivations.

A. Approach

To develop filter tunability, we:

- 1) First derive *separate* expressions for the magnitude and phase of GAFs parameterized by Θ . This is because each of the filter characteristics, Ψ , is defined based on either the magnitude of the transfer function (e.g. peak frequencies, quality factors) *or* its phase (e.g. maximum group delays, phase accumulations) alone.
- 2) Derive expressions for the filter characteristics Ψ in terms of the model constants Θ - i.e. derive expressions $\Psi = f(\Theta)$
- 3) Finally, invert the expressions, $\Psi = f(\Theta)$, to derive expressions for the model constants in terms of filter characteristics - i.e. $\Theta = g(\Psi)$.

Once we have the constants in terms of filter characteristics, $\Theta = g(\Psi)$, we can parameterize GAFs in terms of characteristics, Ψ , rather than in terms of constants, Θ . As mentioned earlier, this tunability is useful for designing GAFs based on desired filter characteristics⁵. We note that the filter design

⁴In the cochlear model from which we obtain the AF expressions, $k(\beta) = k_\beta(\beta) \frac{\beta}{T}$ corresponds to the differential pressure wavenumber and is considered to contain important mechanistic information regarding how we process sounds.

⁵In the context of AFs associated with mechanistic cochlear models, the methods we develop for parameterizing the filter variables in terms of characteristics, also allow us to parameterize mechanistic variables in terms of the same filter characteristics. The parameterization of mechanistic variables in terms of observed filter characteristics allows one to study the relationship between observed characteristics, computed from experimental measurements, and mechanistic variables that are studied scientifically to understand how the auditory system works.

paradigm developed in this paper may be used not only for GAFs, but also other bandpass filters that can be approximated as GAFs near the peak (e.g. equation 4) or dual-band and multi-band filters that can be constructed based on the single-band filters designed here.

B. Transfer Function Magnitude and Phase Expressions

The first step towards developing tunability is to derive the separate expressions for the magnitude and phase of GAFs (\mathbf{P}), as parameterized by the constants Θ . This involves integrating the separate expressions for the real and imaginary parts of the k_β ⁶, due to the relationships,

$$\frac{d}{d\beta} \text{mag}\{\mathbf{P}\} = \frac{20}{\log(10)} \text{Im}\left\{\frac{kl}{\beta}\right\}, \quad (12)$$

and,

$$\frac{d}{d\beta} \text{phase}\{\mathbf{P}\} = -\text{Re}\left\{\frac{kl}{\beta}\right\}. \quad (13)$$

The integrations result in the following expressions for the magnitude and phase of \mathbf{P} , where we use $\text{phase}\{\cdot\}$ to indicate phase in radians and $\text{mag}\{\cdot\} = 20 \log_{10}(|\cdot|)$ to indicate magnitude in dB - to distinguish it from $|\mathbf{P}|$:

$$\begin{aligned} \frac{\log(10)}{20} \text{mag}\{\mathbf{P}(\beta)\} &= -\frac{B_u}{2} \log(A_p^2 + (\beta - b_p)^2) \\ &\quad - \frac{B_u}{2} \log(A_p^2 + (\beta + b_p)^2) \\ &\xrightarrow{\text{sharp-filter approx.}} -\frac{B_u}{2} \log(A_p^2 + (\beta - b_p)^2), \end{aligned} \quad (14)$$

and,

$$\begin{aligned} \text{phase}\{\mathbf{P}(\beta)\} &= -B_u \tan^{-1}\left(\frac{\beta - b_p}{A_p}\right) - B_u \tan^{-1}\left(\frac{\beta + b_p}{A_p}\right) \\ &\xrightarrow{\text{sharp-filter approx.}} -B_u \tan^{-1}\left(\frac{\beta - b_p}{A_p}\right). \end{aligned} \quad (15)$$

In the above equations, we have included sharp-filter approximations in which the second term is negligible compared to the first. The sharp-filter approximation of GAFs results in,

$$\mathbf{P}_{\text{sharp}} = (s - p)^{-B_u}, \quad (16)$$

and, $|\mathbf{P}_{\text{sharp}}| = (A_p^2 + (\beta - b_p)^2)^{-B_u/2}$. The condition for the sharp-filter approximation ($\mathbf{P}(\beta) \approx \mathbf{P}_{\text{sharp}}(\beta)$) is derived in appendix A. While the sharp-filter approximation for GAFs is not physically realizable, it enables us to derive expressions for the filter characteristics, Ψ , in terms of the filter constants, Θ and, consequently, parameterize the GAFs in terms of filter characteristics.

In figure 1, we illustrate the parametric region of validity (in filter constant space) of the sharp-filter approximation for GAFs. We do so by plotting the magnitude and phase of GAF, \mathbf{P} , and of its sharp-filter approximation, $\mathbf{P}_{\text{sharp}}$, as well as plotting the real and imaginary parts of k_β and its sharp-filter approximation. The sharp-filter approximation results in symmetric responses for \mathbf{P} and does not preserve the asymmetry of GAFs. Consequently, we do not include

⁶Integrating the real and imaginary parts of k_β simplifies our derivation immensely due to the fact that we are able to express k_β easily using partial fraction decomposition (equation 11) which leads to simpler individual terms

measures of asymmetry as filter characteristics we use for filter design. In figure 1, we demonstrate the following: (1) For $\text{mag}\{\mathbf{P}\}, \text{Im}\{k_\beta\}$, the sharp-filter approximation is most valid near the peak of \mathbf{P} and for small A_p . Consequently, magnitude-based filter characteristics derived from closest to the peak are most reliable. For instance, $\text{BW}_{15\text{dB}}$ is more reliable than $\text{BW}_{30\text{dB}}$. As A_p increases or as we move away from the peak, the approximation deteriorates, as can be seen in the subplots. (2) On the other hand, for $\text{phase}\{\mathbf{P}\}, \text{Im}\{k_\beta\}$, the sharp-filter approximation is a suitable approximation across β . Consequently, phase-based measures such as group delay are preserved through the approximation.

For AFs (GAFs with filter constant values that mimic auditory signal processing), we find that the sharp-filter approximation is a particularly good approximation in filters that mimic processing up to the human base and apex, and chinchilla base, but less so for the case representing the chinchilla apex which have the same filter order but are not sharp [38], [39]. The sharp-filter approximations make the model more interpretable and are used to determine expressions for $\Psi = f(\Theta)$, and from it, $\Theta = g(\Psi)$, in order to then parameterize the model variables by filter characteristics which serves as the basis for our filter design paradigm.

C. Frequency Domain Filter Characteristics

In the previous section, we derived separate expressions for the magnitude and phase of the filter. The next step towards our characteristics-based filter design paradigm, as described in section III-A, is to derive expressions for the chosen filter characteristics, Ψ , in terms of the filter constants Θ . To do so, we first define our chosen set of frequency domain filter characteristics, then derive $\Psi = f(\Theta)$ using the sharp-filter expressions for magnitude and phase of \mathbf{P} .

The peak (normalized) frequency is defined as,

$$\begin{aligned} \beta_{\text{peak}} &\triangleq \underset{\beta}{\text{argmax}} \text{mag}\{\mathbf{P}(\beta)\} \stackrel{\text{sharp}}{=} b_p \\ &\equiv \underbrace{\frac{1}{\text{CF}(x)} \underset{f}{\text{argmax}} \text{mag}\{\mathbf{P}(f, x)\}}_{\triangleq f_{\text{peak}}}. \end{aligned} \quad (17)$$

which results in $f_{\text{peak}} = \text{CF}(x)$ and $\beta_{\text{peak}} = 1$. Note that we may alternatively have chosen to define a central β based on phase slope criteria instead of magnitude criteria. If we use the sharp-filter approximate expressions, the two definitions for a central β - based on peak magnitude and based on maximum group delay, result in equivalent expressions.

The maximum group delay, N_β , in cycles, is defined as,

$$\begin{aligned} N_\beta &\triangleq \frac{1}{2\pi} \max\left(-\frac{d\text{phase}\{\mathbf{P}\}}{d\beta}\right) \stackrel{\text{sharp}}{=} \frac{1}{2\pi} \frac{B_u}{A_p} \\ &\equiv \text{CF}(x) \underbrace{\frac{1}{2\pi} \max\left(-\frac{d\text{phase}\{\mathbf{P}\}}{df}\right)}_{\triangleq N_f}. \end{aligned} \quad (18)$$

Phase accumulation in cycles (not radians), is,

$$\phi_{\text{accum}} \triangleq -\frac{\max(\text{phase}\{\mathbf{P}\}) - \min(\text{phase}\{\mathbf{P}\})}{2\pi} \stackrel{\text{sharp}}{=} \frac{B_u}{2}, \quad (19)$$

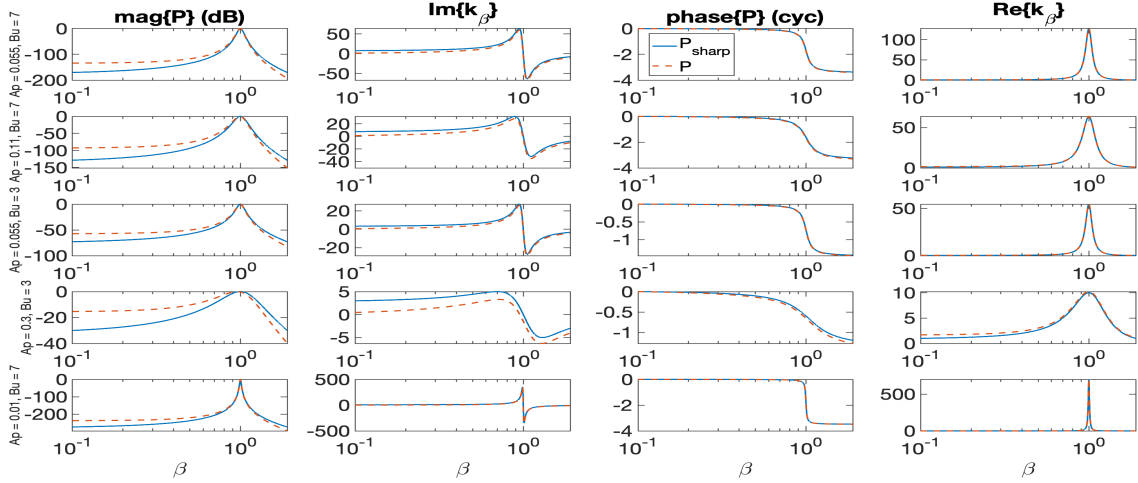


Fig. 1: **Dependence on parameters and validity of sharp-filter approximation:** The figure plots the magnitude and phase of GAF/P and its sharp-filter approximation, \mathbf{P}_{sharp} (normalized to peak magnitude and referenced to zero phase) and real and imaginary parts of k_β as a function of β . Each row is for different values of the model constant, A_p, B_u , with the first two rows having values close to those we expect for AFs mimicking (cumulative) processing by the human base and apex respectively. For all plots, $b_p = 1$. The plots are generated using the equations 9 and 11 for \mathbf{P} and k_β respectively as well as equations 16 and 43 (dashed red lines) for their the sharp-filter approximations, \mathbf{P}_{sharp} and $k_{\beta,sharp}$ (solid blue lines). The two curves are most similar near the peak, and particularly so for sharp filters. Consequently the peak-centric filter characteristics of GAFs can be derived from its sharp-filter approximation. The figure also shows that the dependence of \mathbf{P} magnitude and phase on parameters A_p, B_u is consistent with our expressions for filter characteristics in terms of parameters (section III-C).

and is equivalently defined in both β and f domains. It is the only non-peak-centric measure we take into consideration. The n-dB bandwidth is,

$$\begin{aligned} \text{BW}_{n,\beta} &\triangleq \overbrace{\arg \{ \text{mag}\{\mathbf{P}\}(\beta_{peak}) - \text{mag}\{\mathbf{P}\}(\beta) = n \}}^{\triangleq y_n^+} \\ &\quad - \overbrace{\arg \{ \text{mag}\{\mathbf{P}\}(\beta_{peak}) - \text{mag}\{\mathbf{P}\}(\beta) = n \}}^{\triangleq y_n^-} \\ &\stackrel{\text{sharp}}{=} 2\Delta_n = 2A_p \sqrt{10^{\frac{n}{10B_u}} - 1} \\ &\equiv \frac{1}{\text{CF}(x)} \text{BW}_{n,f}, \end{aligned} \quad (20)$$

where we obtained Δ_n by solving $n = \frac{20}{\log(10)} \left(-\frac{B_u}{2} \log(A_p^2) + \frac{B_u}{2} \log(A_p^2 + \Delta_n^2) \right)$.

The associated quality factor is,

$$\begin{aligned} Q_n &\triangleq \frac{\beta_{peak}}{\text{BW}_{n,\beta}} \stackrel{\text{sharp}}{=} \frac{b_p}{2A_p} \left(10^{\frac{n}{10B_u}} - 1 \right)^{-\frac{1}{2}} \\ &\equiv \frac{f_{peak}}{\text{BW}_{n,f}}, \end{aligned} \quad (21)$$

which is equivalent regardless of whether it is defined in the β or f domains.

The equivalent rectangular bandwidth (ERB) is,

$$\begin{aligned} \text{ERB}_\beta^{(\beta_1, \beta_2)} &\triangleq \frac{1}{|\mathbf{P}(\beta_{peak})|^2} \int_{-\beta_1}^{\beta_2} |\mathbf{P}(\beta)|^2 d\beta \\ &\stackrel{\text{sharp}, (-\infty, \infty)}{=} \frac{1}{\sqrt{\pi} A_p} \frac{\Gamma(B_u - \frac{1}{2})}{\Gamma(B_u)} \\ &\equiv \frac{1}{\text{CF}(x)} \underbrace{\frac{1}{|\mathbf{P}(\beta(f_{peak}, x))|^2} \int_{-f_1}^{f_2} |\mathbf{P}(f, x)|^2 df}_{\triangleq \text{ERB}_f^{(f_1, f_2)}}. \end{aligned} \quad (22)$$

The limits of integration are relevant when numerically estimating the ERB from data over a finite domain. The ERB we derive from analytic expressions is $\text{ERB}_\beta^{(-\infty, \infty)}$. To derive our expression for ERB, we first evaluate the indefinite integral which results in Gauss Hypergeometric Functions (GHF), ${}_2F_1(a, b; c; z)$ with $z = -\left(\frac{\beta - b_p}{A_p}\right)^2$. We then express this in terms of GHFs in z^{-1} , and then expand those GHFs around zero to determine the expressions at $\beta = \infty, -\infty$. Details are included in appendix B.

The associated quality factor is,

$$\begin{aligned} Q_{erb} &\triangleq \frac{\beta_{peak}}{\text{ERB}_\beta} \stackrel{\text{sharp}}{=} \frac{b_p}{\sqrt{\pi} A_p} \frac{\Gamma(B_u)}{\Gamma(B_u - \frac{1}{2})} \approx \frac{e^b b_p B_u^{1-a}}{2\pi A_p} \\ &\equiv \frac{f_{peak}}{\text{ERB}_f} \end{aligned} \quad (23)$$

which is equivalent in both β and f domains. The approximation is valid for relevant B_u values (and for all A_p, b_p values), with fixed values for $b = 1.02, a = 0.418$.

We introduce an additional magnitude-based filter characteristic, S_β , that may be considered a more peak-centric measure of bandwidth. We define S_β in decibels as:

$$\begin{aligned} S_\beta &\triangleq - \left. \frac{d^2 \text{mag}\{\mathbf{P}(\beta)\}}{d\beta^2} \right|_{\beta_{peak}} \stackrel{\text{sharp}}{=} \frac{20}{\log(10)} \frac{B_u}{A_p^2} \\ &\equiv - \underbrace{\left. \frac{d^2 \text{mag}\{\mathbf{P}(\beta(f_{peak}, x))\}}{df^2} \right|_{f_{peak}}}_{\triangleq S_f} \text{CF}(x)^2. \end{aligned} \quad (24)$$

As A_p decreases, the filters become sharper resulting in an increased S_β , and equivalently, decreased $\text{BW}_{n,\beta}$ and ERB. While S_β is very useful for specifying desired peak-centric filter behavior, we note that it is not appropriate to compute

this characteristic from measured data of filter transfer functions (at least not without smoothing) due to noise issues that are compounded by taking derivatives in equation 24.

In this section, we have defined the frequency-domain filter characteristics of interest, Ψ , and derived their expressions in terms of the model constants Θ using the sharp-filter expressions for magnitude and phase of GAFs. These expressions, $\Psi = f(\Theta)$, are summarized in table I. Note that our definitions for ϕ_{accum} , Q_n , Q_{erb} are the same in f and β domains. The other characteristics, β_{peak} , $BW_{n,\beta}$, ERB_β , N_β , S_β are easily converted into their counterparts in the frequency domains ⁷.

	Filter Characteristics	Expression in Terms of Model Constants
I.1	$\beta_{peak} = \frac{1}{CF(x)} f_{peak}$	b_p
I.2	$N_\beta = CF(x) N_f$	$\frac{1}{2\pi} \frac{B_u}{A_p}$
I.3	ϕ_{accum}	$\frac{B_u}{2}$
I.4	Q_n	$\frac{b_p}{2A_p} (10^{\frac{n}{10B_u}} - 1)^{-\frac{1}{2}}$
I.5	Q_{erb}	$\frac{b_p}{\sqrt{\pi} A_p} \frac{\Gamma(B_u)}{\Gamma(B_u - \frac{1}{2})} \approx \frac{e^{b_p B_u^{1-a}}}{2\pi A_p}$
I.6	$S_\beta = CF^2(x) S_f$	$\frac{20}{\log(10)} \frac{B_u}{A_p^2}$

TABLE I: **Frequency-domain filter characteristics in terms of model constants** $\Psi = f(\Theta)$. The filter characteristics without a β or f subscript are equal in both domains. The expressions are derived from the sharp-filter approximations of the filter transfer function magnitude and phase. The constants for Q_{erb} take on the following values, $b = 1.02$, $a = 0.418$.

Figure 1 shows that the dependence of \mathbf{P} magnitude and phase on parameters A_p, B_u is consistent with our above expressions (table I) for filter characteristics in terms of filter constants. Specifically, the figure show that the parameters control the behavior of the pressure filter as follows: phase accumulation increases with B_u , the maximum group delay increases with B_u and decreases with A_p , sharpness of tuning decreases with A_p and increases with B_u . We note that the behavior of V , particularly near the peak, is dominated by \mathbf{P} , and hence the dependence of its behavior on model constants is similar to that of \mathbf{P} .

D. Parameterizing the Model in Terms of Filter Characteristics

In section III-C, we derived filter characteristics in terms of the model constants, $\Psi = f(\Theta)$. The final step towards parameterizing the GAFs in terms of filter characteristics (as per section III-A), is to invert sets of these expressions to express the filter constants, Θ , as functions of subsets of Ψ . Our derived parameterizations of Θ in terms of various possible combinations of the filter characteristics (including mixed magnitude-based and phase-based characteristics) is in table II. These parameterizations/inversions are possible due to the simplicity of expressions in table I derived using the sharp-filter approximation. One particularly important combination

⁷We previously explained the significance of using β rather than f for filterbanks with constant-Q filters (see section II). For scientific studies of cochlear models associated with AFs, we note that while reported values for filter characteristics based on measured data are in the frequency domain, rather than in the normalized frequency domain, the inherent variation of properties along the length of the cochlea lead to characteristics, such as bandwidths and group delays, that when defined in the β domain may be considered constant at least locally. In our model, this slow variation of characteristics is captured in the local scaling symmetry of k , and our assumptions regarding C .

is in terms of the set of characteristics: β_{peak}, N, Q_{erb} , which allows one to design sharp filters while introducing limited delay.

Based on the expressions in table II, we may consider $b_p = 1$ as a fixed parameter. We may use appropriate combinations of two other characteristics for determining A_p, B_u . Note that table II only includes a subset of such possible parameterizations. For instance, we may use the compound characteristics, $\frac{Q_{erb}}{Q_{10}}$ or $\frac{Q_3}{Q_{10}}$, which are purely a function of B_u as part of our filter design paradigm serving as an alternative to ϕ_{accum} or $\frac{Q}{\beta_{peak} N}$ for determining B_u . This allows for parameterizing the filter in terms of a set of only magnitude-based characteristics. However, for anticipated values of B_u , we find that $\frac{Q_{erb}}{Q_{10}}$ is less sensitive to variations in B_u compared to ϕ_{accum} and $\frac{Q}{\beta_{peak} N}$.

In the case of AFs, $\frac{Q_{erb}}{Q_{10}}$ is particularly relevant as previous work has found that $1.7 \geq \frac{Q_{erb}}{Q_{10}} \geq 1.8$ which results in the condition $B_u > 3.85$ for all AFs ⁹.

As an example of parameterizing the GAFs in terms of filter characteristics, we consider the parameterization in terms of $\beta_{peak}, N, \phi_{accum}$ which results in the poles being $-\frac{\phi_{accum}}{\pi N} + i\beta_{peak}$, and the filter order being $-2\phi_{accum}$, or equivalently,

$$\mathbf{P}(s) = \left(s^2 + 2\frac{\phi_{accum}}{\pi N} s + \beta_{peak}^2 + \left(\frac{\phi_{accum}}{\pi N} \right)^2 \right)^{-2\phi_{accum}}. \quad (25)$$

E. Testing for AFs

Elsewhere in this paper, we derived the condition for validity of the sharp-filter approximation (appendix A) and illustrated the similarity of the magnitude and phase of GAFs, $\mathbf{P}(\beta)$, and the sharp-filter approximation for GAFs, $\mathbf{P}_{sharp}(\beta)$ (figure 1). We then presented expressions to parameterize $\mathbf{P}(\beta)$ in terms of the filter characteristics, Ψ , that we derived based on our expressions for $\mathbf{P}_{sharp}(\beta)$ (not $\mathbf{P}(\beta)$) which we assumed is an appropriate approximation. In this section we assess the validity of this assumption by comparing the following two sets of filter characteristics, Ψ :

- 1) $\Psi_{desired}$ which were derived from $\mathbf{P}_{sharp}(\beta)$ and used to parameterize and generate $\mathbf{P}(\beta)$
- 2) $\Psi_{num,P}$ which is numerically computed (according to the basic definitions in section III-C) from $\mathbf{P}(\beta)$ after it has been designed from $\Psi_{desired}$

Specifically, we define the relative error in each of the filter characteristics as,

$$\epsilon_\Psi = \frac{\Psi_{desired} - \Psi_{num,P}}{\Psi_{desired}}. \quad (26)$$

In figure 2, we demonstrate the relative errors in Q_{erb} and N_β as a function of desired values for Q_{erb} and N_β (while holding $\beta_{peak} = 1$). We find that ϵ_Ψ is relatively small for the range of desired filter characteristics which were chosen to satisfy the condition for the sharp-filter approximation.

We also graph the relative errors between desired and computed filter characteristics, ϵ_Ψ , for a variety of filter

⁹These estimates are from experiments across various species and locations along the length of the cochlea [40]. This results in $B_u > 3.85$ as a constraint across species and locations.

	Θ expressions	b_p	A_p	B_u
II.1	$\beta_{peak}, N, \phi_{accum}$	β_{peak}	$\frac{\phi_{accum}}{\pi N}$	$2\phi_{accum}$
II.2	β_{peak}, N, Q_{erb}	β_{peak}	$= \frac{1}{2\pi N} B_u$ or, $= \frac{\beta_{peak}}{\sqrt{\pi} Q_{erb}} \frac{\Gamma(B_u)}{\Gamma(B_u - \frac{1}{2})}$	$\approx e^{\frac{b}{a}} \left(\frac{Q_{erb}}{\beta_{peak} N} \right)^{-\frac{1}{a}}$
II.3	$\beta_{peak}, Q_{erb}, \phi_{accum}$	β_{peak}	$\frac{\beta_{peak}}{\sqrt{\pi} Q_{erb}} \frac{\Gamma(2\phi_{accum})}{\Gamma(2\phi_{accum} - \frac{1}{2})}$	$2\phi_{accum}$
II.4	$\beta_{peak}, Q_n, \phi_{accum}$	β_{peak}	$\frac{\beta_{peak}}{2Q_n} \left(10^{20\phi_{accum}} - 1 \right)^{-\frac{1}{2}}$	$2\phi_{accum}$
II.5	β_{peak}, S_β, N	β_{peak}	$\frac{40\pi}{\log(10)} \frac{N}{S_\beta}$	$\frac{80\pi^2}{\log(10)} \frac{N^2}{S_\beta}$
II.6	$\beta_{peak}, S_\beta, \phi_{accum}$	β_{peak}	$\sqrt{\frac{40\pi}{\log(10)} \frac{\phi_{accum}}{S_\beta}}$	$2\phi_{accum}$
II.7	β_{peak}, Q_n, N	β_{peak}	$\frac{1}{2\pi N} B_u$	solve the implicit equation $\frac{Q_n}{\beta_{peak} N} = \frac{\pi}{B_u} \left(10^{10\frac{n}{B_u}} - 1 \right)^{-\frac{1}{2}}$

TABLE II: Model constants in terms of desired or measured filter characteristics $\Theta = \mathbf{g}(\Psi)$. Γ is the gamma function, and $a = 0.418, b = 1.02$. Note that our parameterizations allow for dictating both magnitude-based and phase-based filter characteristics

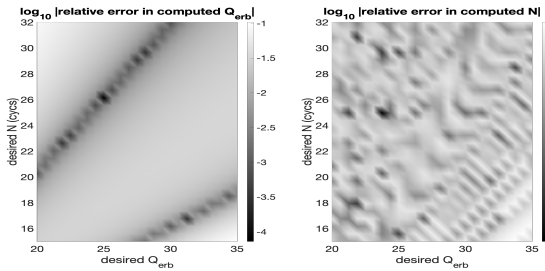


Fig. 2: The relative error in filter characteristics introduced due to using the approximation is small: The error in computed Q_{erb} (left) and N (right) relative to the desired values for these characteristics are shown as a function of desired values for Q_{erb} and desired N ($\beta_{peak} = 1$ throughout). This figure is used to demonstrate the accuracy of the filter design method - as can be deduced from the range of values (in the colorbar), rather than to demonstrate any error pattern.

characteristics in the bottom panel of figures 3 and 4, (middle, red bars) for the various filter characteristics. Each of these figures is generated using a different set of desired filter characteristic values. Comparing figures 3 and 4 illustrates that the relative errors in characteristics is smaller for sharper filters.

The relative errors in magnitude-based filter characteristics are small because these characteristics are peak-centric (e.g. $BW_{n,\beta}, S_\beta$) or weigh the peak region far more than it does the skirts (e.g. ERB). The relative error in N_β is particularly negligible as expected from phase-based characteristics which are nearly identical for \mathbf{P} and \mathbf{P}_{sharp} . The relative error in ϕ_{accum} is larger than expected, but this is due to the fact that $\phi_{accum,num,P}$ is computed from a finite range of β . This becomes clear when we compute a relative error between desired filter characteristics and that computed from \mathbf{P}_{sharp} constructed from the desired characteristics: $\frac{\Psi_{desired} - \Psi_{num,Psharp}}{\Psi_{desired}}$ (notice the use of P_{sharp} rather than P in the subscript of the computed characteristics). This relative error (left, blue bars in figures 3 and 4) is very nearly the same as that for the phase accumulation for \mathbf{P} , supporting our argument that the reason behind the error in phase accumulation is synthetic and due to finite ranges of β in computation rather than a true error.

The related filter, \mathbf{V} may, to first approximation, also be

designed using the filter-characteristic-based parameterization derived from \mathbf{P}_{sharp} and does not require rederiving filter-characteristic-based parameterization specifically for \mathbf{V} . In the top panels of figures 3 and 4, we show the similarity between \mathbf{P} and \mathbf{V} near the peak. We may define relative errors between $\Psi_{desired}$ (used to design both \mathbf{P} and \mathbf{V}) and $\Psi_{num,V}$ which we compute numerically from the generated transfer functions for V using the definitions of section III-C. The relative errors in certain filter characteristics for V - $\beta_{peak}, \frac{Q_{erb}}{Q_{10}}, \frac{Q_{10}}{N}, \frac{Q_{erb}}{N}$ (all of which are independent of A_p), are smaller than others.

The relative errors in characteristics from the constructed \mathbf{V} (right, yellow bars in figures 3 and 4) may be considered small but are much larger than the negligible relative errors in characteristics from the constructed \mathbf{P} (middle, red bars in the figures). This is expected as the filter characteristics used to design them were developed using the sharp-filter approximate expressions for \mathbf{P} and not \mathbf{V} (see section III).

F. Testing for Second Order Systems

Here we test our derived expressions, $\Theta = f(\Psi)$ and the characteristics-based parameterization of GAFs using the particular case of $B_u = 1$ which occurs in the classically studied second order systems. As previously mentioned, we are only interested in ranges of parameter values for which the system acts as a bandpass filter, and hence the set of filter characteristics derived in this paper can all be properly defined.

For AFs - the special case of GAFs discussed in the previous section, $B_u \geq 2$ for integer B_u , based on the behavior of impulse responses that mimic cochlear signal processing. In contrast, for the case of $B_u = 1$, the GAF reduces to a rational transfer function with a pair of complex conjugate poles characteristic of various second order systems including forced damped harmonic oscillators (such as mass-spring-dashpot systems with displacement as the dependent variable, and certain configurations of RLC circuits). As far as filter representations are concerned, these may be considered a special case of GAFs (equation 3). Second order systems can be represented as,

$$H(s) \propto \frac{1}{(s-p)(s-\bar{p})} = \frac{1}{s^2 + 2as + (a^2 + b^2)}, \quad (27)$$

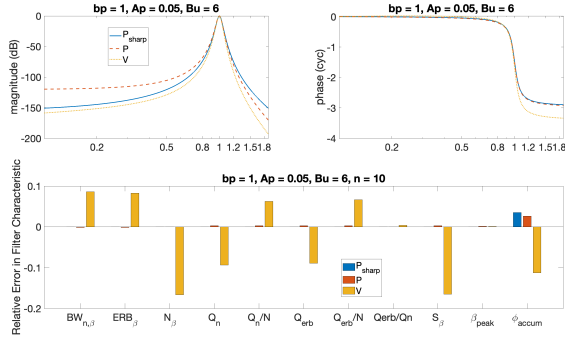


Fig. 3: The relative error in filter characteristics introduced due to using the approximation is small: Using specified values for filter characteristics, $\Psi_{desired}$, we generate $\mathbf{P}_{sharp}(\beta)$, $\mathbf{P}(\beta)$, $\mathbf{V}(\beta)$. This figure was generated using filter constant values as per the figure title, or equivalently, using a subset of the following desired values for filter characteristics, $\Psi_{desired}$: $\beta_{peak} = 1$, $N_{\beta} = 19.1$ cyc, $\phi_{accum} = 3$ cyc, $Q_{erb} = 25.9$, $ERB_{\beta} = 0.039$, $Q_{10} = 14.6$, $BW_{10,\beta} = 0.69$, $S_{\beta} = 2.08 \times 10^4$ dB, $\frac{Q_{erb}}{N} = 1.35$ cyc $^{-1}$, $\frac{Q_{10}}{N} = 0.77$ cyc $^{-1}$, $\frac{Q_{erb}}{Q_{10}} = 1.77$. The magnitudes and phases (top) illustrate similarity near the peak, thereby supporting our choice of parameterizing \mathbf{P} and \mathbf{V} using peak-centric filter characteristics of \mathbf{P}_{sharp} . The bottom graph shows that the relative errors in Ψ between the desired filter characteristics and those computed from the generated transfer functions. This is done for \mathbf{P}_{sharp} (left, blue bars), \mathbf{P} (middle, red bars), and \mathbf{V} (right, yellow bars). We find that the relative error is small for values of filter characteristics we use. An accompanying figure with an alternate set of filter characteristic values for parameterization is figure 4.

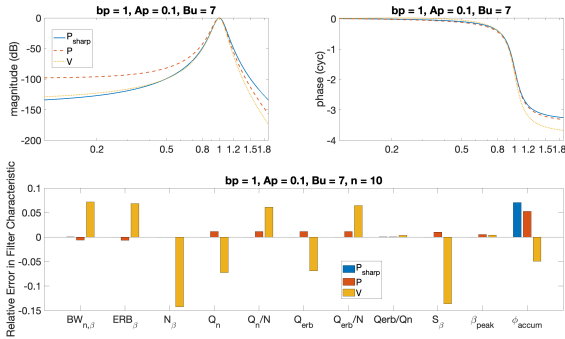


Fig. 4: The relative error in filter characteristics introduced due to using the approximation is small: See figure 3 for a full description. This figure was generated using filter constant values (in the figure titles) corresponding to the following values of desired filter characteristic $\Psi_{desired}$: $\beta_{peak} = 1$, $N_{\beta} = 11.1$ cyc, $\phi_{accum} = 3.5$ cyc, $Q_{erb} = 14.1$, $ERB_{\beta} = 0.071$, $Q_{10} = 8$, $BW_{10,\beta} = 0.12$, $S_{\beta} = 6.08 \times 10^3$ dB, $\frac{Q_{erb}}{N} = 1.27$ cyc $^{-1}$, $\frac{Q_{10}}{N} = 0.72$ cyc $^{-1}$, $\frac{Q_{erb}}{Q_{10}} = 1.76$. Note that the filter is less sharp than that in figure 3 and so the relative errors in the pressure filter characteristics (middle, red bars) due to deviation from the sharp-filter condition are larger.

with $p = -a + ib$ (to make it close to our previous notation with $p = -A_p + ib_p$), and s being the classical Laplace- s . We may equivalently express this using the more common convention,

$$H(s) \propto \frac{1}{s^2 + 2\zeta\omega_n s + \omega_n^2}, \quad (28)$$

where we may relate the two sets of filter constants as follows:

$$\begin{cases} a = \zeta\omega_n \\ b = \sqrt{\omega_n^2 - a^2} = \omega_n \sqrt{1 - \zeta^2}. \end{cases} \quad (29)$$

Clearly, the filter representation in equation 27 for second order systems is simple enough that we can compare the expressions for filter characteristics from the literature with the expressions we obtained using the sharp-filter approximation. This allows us to test the validity of expressions $\Psi = f(\Theta)$ (and consequently of $\Theta = g(\Psi)$) using the special case of $B_u = 1$.

We first list the expressions for filter characteristics for second order systems using our derived expressions in table I. We then provide the expressions for filter characteristics as derived in the literature from equation 27. Finally, we compare the two sets of expressions for sharp-filters as a test of our expressions $\Psi = f(\Theta)$.

1) *Using Our Expressions:* Using our expressions for the peak frequency, quality factor, phase accumulation and group delay (table I), we arrive at the following set of expressions for filter characteristics for the case of $B_u = 1$. Note that we use our equations in the β domain as the expressions for ω due to our switching the definition of s to the Laplace- s in this section. Hence, the expressions in normalized frequency β in the previous sections map directly to expressions in angular frequency ω here. For example, the peak is at $\omega_{peak} = \text{argmax} |H(i\omega)|$, and the group delay at the peak is $N = -\frac{1}{2\pi} \frac{d\text{phase}\{H(i\omega)\}}{d\omega} \Big|_{\omega=\omega_{peak}}$.

$$\omega_{peak} = b = \omega_n \sqrt{1 - \zeta^2} \quad (30)$$

$$N = \frac{1}{2\pi a} = \frac{1}{2\pi \zeta \omega_n} \quad (31)$$

$$\phi_{accum} = \frac{1}{2} \quad (32)$$

$$Q_3 = \frac{b}{2a\sqrt{10^{3/10} - 1}} \approx \frac{b}{2a} = \frac{\sqrt{1 - \zeta^2}}{2\zeta} \quad (33)$$

The sharp-filter condition presented in appendix A is practically,

$$a < 0.2 \implies \zeta\omega_n < 0.2. \quad (34)$$

Implicit in, and preceding this condition, is the presumption that the filter is bandpass - has a real, nonzero, peak frequency and a real, finite value, for its bandwidth, and the other conditions that must be fulfilled to making it so.

2) *Using Classical Expressions:* Below, we list expressions from the literature for filter characteristics of second order systems. There are several conditions for this bandpass property of driven systems beyond the underdamped condition, $\zeta < 1$ (which results in a solution to the homogeneous equation to oscillate at $\omega_n \sqrt{1 - \zeta^2}$), which we mentioned below.

The first filter characteristic is peak frequency,

$$\omega_{peak} = \omega_n \sqrt{1 - 2\zeta^2}. \quad (35)$$

The parameter values are additionally restricted at this stage as resonance phenomenon only occurs for significantly underdamped systems,

$$\zeta < \frac{1}{\sqrt{2}}, \quad (36)$$

which is the condition for the ω_{peak} expression. The generally seen approximation in which the resonant frequency is approximated by that of the undamped oscillator,

$$\omega_{peak} = \omega_n, \quad (37)$$

is only appropriate for lightly damped oscillators - i.e. when ζ is much smaller than this value,

$$\zeta \ll 1 \quad (38)$$

The next two filter characteristics are the group delay at the peak, and the phase accumulation in radians are expressed in classical literature as,

$$N = \frac{1}{2\pi\zeta\omega_n}, \quad (39)$$

and,

$$\phi_{accum} = \frac{1}{2}. \quad (40)$$

Lastly, Q_3 is constructed from BW_3 . The existence of BW_3 invokes a stronger condition than that of the resonant condition¹⁰. However, this condition is much less restrictive than the lightly damped condition in equation 38. For lightly damped oscillators, the half-power quality factor may be approximated as,

$$Q_3 = \frac{1}{2\zeta} \quad (41)$$

3) *Testing our expressions:* The two expressions for N and ϕ_{accum} (that in classical literature and that derived here using the sharp-filter approximation) are identical. For the case of lightly damped systems, the expressions for the remaining filter characteristics are also identical. This gives credence to our derived expressions for filter characteristics in terms of filter constants and consequently, our expressions for the filter constants in terms of filter characteristics used to parameterize the filters.

IV. EXTENSION TO MULTI-BAND FILTERS

One method for designing dual-band and multi-band filters involves expressing these filters as the sum of single-band filters [32]. Consequently, our filter design method may be used for the design of multi-band filters that have distinct peaks (rather than flat passbands) provided that the constitutive single-band filters may be represented as GAFs or related filters.

In figure 5, we exemplify the frequency responses of multi-band filters constructed via the summation of constitutive GAFs that were designed using desired values for various

sets of magnitude-based filter characteristics. We note that the choice of filter characteristics that may be used to design multi-band filters depends on the proximity of the peaks to one another. For instance, Q_3 may be better used in the design of multi-band filters compared with Q_{10} particularly if the frequency responses of the constitutive single-band filters have more overlap. The most peak-centric of the magnitude filter characteristics, S_β , is the least restrictive in terms of requirements on peak-proximity and shape. Taking these observations into consideration when choosing the appropriate set of filter characteristics to design multi-band filters results in low values of relative errors as shown in figure 5. Future directions include deriving mathematical conditions for the applicability of our single-band filter design methods for various cases of multi-band filters.

V. CONCLUSIONS AND FUTURE DIRECTIONS

We have developed direct and non-iterative filter design methods for GAFs and related bandpass and multi-band filters. We do not use analog prototype filters (which have set predetermined frequency response shapes) such as Butterworth and Chebychev, but instead develop methods for an alternative class of filters. Our problem also diverges from existing analog-prototype-based methods for IIR filter design in that we are not dealing with filters with a flat passband and cut-off frequencies. Instead, the filters we are concerned with have a clear peak. Additionally, our objective is designing the filter based on specified values for filter characteristics.

We derived parameterizations for GAFs in terms of frequency domain filter characteristics including quality factors and group delays. This enables easy and direct tuning of the filters based on desired values for characteristics. This is in contrast to current filter design paradigms for GAFs (with the exception of second order systems) with which one is constrained to a single set of values or must search through filter constant values to get the desired filter behavior. It is also in contrast to most current filter design methods for other classes of filters in which the frequency response, rather than simply desired filter characteristics, is used. Consequently, in designing the filters, we must specify only three values (characteristics) rather than an array of values at various frequencies. Our filter design methods are developed in continuous frequency and the filters can then directly be converted into digital filters using the usual analog to digital transformation methods such as the bilinear transform. We note that the filter design methods developed here are not only useful for digital filters, but may be directly used in designing analog circuits as well. Future work involves equivalent representations and formulations, including a fractional-calculus based formulation for rational filter order, so that one is not restricted to direct transfer function representations.

A. Filter Design Paradigm

The filter design paradigm that we developed can be used for approximate filter-characteristic-based parameterizations (or filter constant estimation) of other classes of bandpass

¹⁰and the existence of BW_6 imposes an even more stringent condition

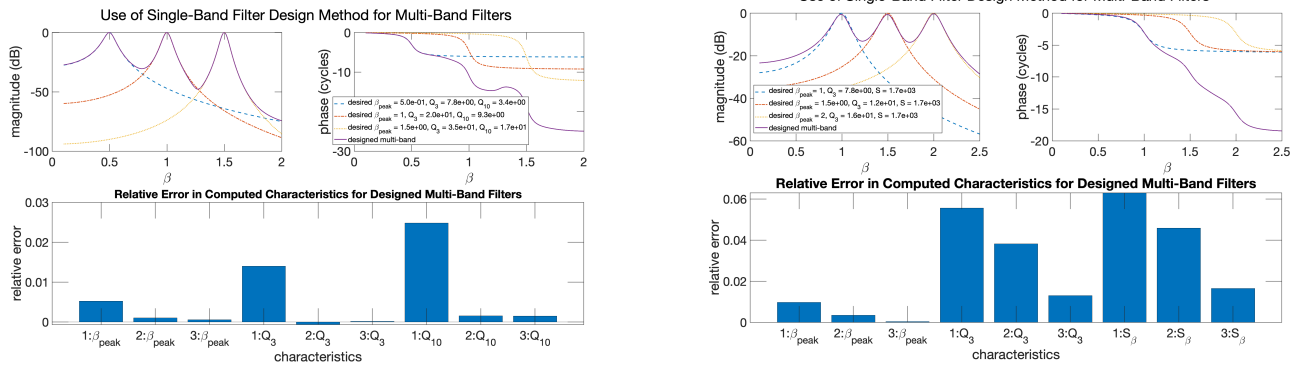


Fig. 5: The characteristics-based filter design method may be used for certain multi-band filters: The multi-band filter (solid lines in top figure) is designed by summing the transfer functions of individual GAFs (dashed, dash-dotted, and dotted lines) which are in turn designed using specific values for the filter characteristics - β_{peak} , Q_3 , Q_{10} (left) and β_{peak} , Q_3 , S_β (right). The relative error in the filter characteristics of the multi-band filter is shown in the bottom bar graphs.

filters. We consider this an analytic deterministic frequency-characteristic-based form of filter design, which may be derived for certain other bandpass filters used in signal processing and might further be developed for 2D bandpass filters such as those useful in image processing. Our filter design methods are also directly useful for related bandpass filters (e.g. equation 4) and associated multi-band filters where it can be used to directly and accurately dictate the desired bandwidths associated with each peak. Additionally, it may be of interest to extend the characteristics-based filter design method for associated low-pass and high-pass filters as well as bandstop filters - especially notch filters for which fine control over the valley is desired. Finally, it is of interest to develop characteristics-based filter design methods for the digital filters corresponding to digital counterparts to GAFs, as well as of other digital filters.

B. Parameterized GAFs

In this paper, we have specifically developed methods for filter design and derived parameterizations of the GAFs in terms of certain frequency domain transfer function characteristics including phase-based characteristics such as group delay. Importantly, the parameterization allows for dictating peak frequencies, bandwidths, and group delays at the peak all simultaneously which is very powerful. This allows for designing sharply tuned filters without significant delay. Additionally, the ability to dictate both magnitude-based and phase-based filter characteristics is particularly important for filterbanks in which synchrony and frequency selectivity is especially important. The tunable filterbanks may particularly prove useful in speech processing, and communication systems. Our expressions may also be very useful in designing circuits (whether electric or otherwise) with specified bandpass properties, f_{peak} , Q , N .

In section I, we stated that a variety of applications might benefit from easily tunable GAFs or corresponding tunable filterbanks. Future directions involve pursuing some of these applications, which in turn may require alternate parameterizations, selecting appropriate values for desired characteristics, further developing implementations, or incorporating certain

features (e.g. orthogonality) in equivalent representations. Accurate and direct filter design paradigms will enable maximizing information obtained from each of these processed signals easily. The ability to parameterize the filters to directly control their behavior (as is the case with the characteristic-based filter design paradigm proposed here) would allow us to better tune, and personalize, filters for their intended applications. For instance, they may aid in developing compensators for those with certain peripheral hearing pathologies upon determining optimal signal synthesis from the filterbanks. We expect that the parameterizations we derived for filter design may be useful for tunable multi-resolution modeling and signal processing.

C. Alternative Filter Characteristics

Future work may involve parameterizations using other relevant frequency domain characteristics such as the asymmetry of transfer function magnitudes. Additionally, it may be desirable to derive expressions for the filter constants in terms of time domain impulse or step response filter characteristics such as settling time, instantaneous frequency, and parameters of envelope shape. These expressions would be useful for easily tuning the GAFs based on desired time domain characteristics. In the context of AFs and associated cochlear models, the combination of parameterizations using time domain and frequency domain characteristics provides a mapping between characteristics in the time domain and those in the frequency domain which would be useful for building intuition and a common framework for interpreting experiments in different domains.

D. Scientific Studies Using Tunable AFs and Associated Cochlear Models

The parameterizations is useful not only for signal processing applications, but can also be used for scientific studies investigating how the cochlea works and for perceptual studies. This is due to the fact that a subset of the GAFs (the AFs) have an underlying mechanistic model [34]. For instance, the characteristics-based parameterization may be used for perceptual studies in which certain filters along the length of

the cochlea deviate from their normal filter characteristics, and we wish to study the effects on perceptual processing. In this case, we associate these changes in perceptual function with changes in filter characteristics.

The parameterization presented here may be useful for pursuing scientific studies of how the cochlea works which is enabled by the physics-based equations at the core of the model associated with AFs, as well as its simplicity and parametrizability. Of particular interest is determining the relationship between characteristics of the filter variables (e.g. quality factors, group delays, peak frequencies), and mechanistic properties such as nominal stiffness and slope of negative damping and gain features, or indeed more interesting properties such as those relating to power flux into the traveling wave. Additionally, it is of interest to identify which filter properties (including filter order) vary with species and location and which may be considered species-invariant, and then determine implications in terms of species or location-independent mechanisms.

APPENDIX A

SHARP-FILTER APPROXIMATION AND CONDITIONS

A. Derivation

From equation, 11, we may express the real and imaginary parts of the k_β separately as follows¹¹.

$$\begin{aligned} \text{Im}\{k_\beta\} &= \frac{1}{A_p^2} \frac{-B_u(\beta - b_p)}{1 + (\frac{\beta - b_p}{A_p})^2} + \frac{1}{A_p^2} \frac{-B_u(\beta + b_p)}{1 + (\frac{\beta + b_p}{A_p})^2} \\ &\xrightarrow{\text{sharp-filter approx.}} \frac{-B_u(\beta - b_p)}{A_p^2 + (\beta - b_p)^2}, \\ \text{Re}\{k_\beta\} &= \frac{1}{A_p^2} \frac{B_u A_p}{1 + (\frac{\beta - b_p}{A_p})^2} + \frac{1}{A_p^2} \frac{B_u A_p}{1 + (\frac{\beta + b_p}{A_p})^2} \\ &\xrightarrow{\text{sharp-filter approx.}} \frac{B_u A_p}{A_p^2 + (\beta - b_p)^2}. \end{aligned} \quad (42)$$

Recall that $\beta > 0$ and the parameters B_u, b_p, A_p take on positive, real, values. For AFs, generally $b_p \approx 1, A_p < 1, B_u \geq 2$. These separate expressions are then used to derive the expressions for the magnitude and phase of P - see equations 14 and 15, (as P is defined as the exponent of the integral of the k_β).

We may also express the complex k_β as follows - corresponding to the sharp-filter approximation of equation 11,

$$k_\beta \xrightarrow{\text{sharp-filter approx.}} B_u \frac{1}{s - p}. \quad (43)$$

The above approximation leads to simple, interpretable counterparts to the full expressions, and enables us to invert filter characteristic expressions for parameters (which is needed for tunability). Note, however, that the approximations result in magnitudes for $\mathbf{P}_{sharp}(\beta)$ that are symmetric whereas the full expression, \mathbf{P} , is asymmetric. Additionally, the sharp-filter approximation results in filters that are not physically realizable. Consequently, we use the approximation to develop tunability and parameterize the GAFs in terms of filter characteristics,

¹¹In the corresponding mechanistic cochlear model $k_\beta = k \frac{1}{\beta}$ denotes the dimensionless wavenumber which describes propagation in the transformed space β , where k is the wavenumber in x .

but use the full expression to generate the process signals and generate responses.

B. Behavior

The above sharp-filter expressions for $\text{Re}\{k_\beta\}$ and $\text{Im}\{k_\beta\}$ - equation 42, directly provide much information regarding the behavior of P and its dependence on the parameters A_p, b_p, B_u :

- b_p determines the β at which the zero crossing of $\text{Im}\{k_\beta\}$ and the maximum of $\text{Re}\{k_\beta\}$ occur, which in turn determine the β at which both the peak in $|P|$ and maximum group delay occur
- B_u, A_p determine the shape (widths and slopes) and scale of the magnitude and phase. This is better seen by noting that B_u, A_p both determine the magnitude of $\text{Im}\{k_\beta\}, \text{Re}\{k_\beta\}$ at any particular β away from the peak (which corresponds to sharpness of $|P|$ and gradient of ϕ_P respectively)
- B_u determines the phase accumulation
- $\frac{B_u}{A_p}$ determines the maximum group delay (which is determined by the value of $\text{Re}\{k_\beta\}$ at the peak of $|P|$)

C. Condition for Sharp-Filter Approximation

The criteria for validity of the sharp-filter approximation depends on the values of $\beta, b_p, A_p, A_p, B_u$. In equation 42, $\frac{|\beta - b_p|}{A_p} < \frac{|\beta + b_p|}{A_p}$ is always true. Hence, the first term generally dominates. As this is especially true near the peak, the sharp-filter approximation is most accurate near the peak. Furthermore, the second term goes to zero much faster than the first if $\frac{|\beta + b_p|}{A_p} \gg 1$. Consequently, the condition is $A_p \ll \beta + b_p$, which at the peak (when $\beta = b_p$) is simply, $A_p \ll 2b_p$. In other words, $A_p \ll 2$. Practically, this is quite suitable for $A_p < 0.2$. The sharp-filter approximation is more appropriate for $\text{Re}\{k_\beta\}$ and parts of variables derived from it (e.g. phase of \mathbf{P}) than the imaginary part due to the nature of their respective numerators in equation 42.

The condition on sharp-filter approximation may alternatively be determined from equations 11 and 43. From these expressions, it is clear that the sharp-filter approximation is valid when $|s - \bar{p}| \gg |s - p|$ (i.e. A_p is small or $\alpha \triangleq \frac{A_p}{\beta + b_p} \ll 1$). Near the peak of P (i.e. near $\beta \approx b_p$), the sharp-filter condition is simply $\frac{A_p}{2b_p} \ll 1$. This is consistent with our description in the previous paragraphs.

APPENDIX B

DERIVATION OF ERB AND Q_{erb} EXPRESSIONS

Here we derive our expressions for ERB (equation 22) and associated quality factor (23) in terms of the model constants, Θ .

The ERB, as defined in section III-C may be expressed as,

$$\text{ERB}_\infty = \frac{1}{|P_{max}|^2} I_\infty, \quad (44)$$

with,

$$|P_{max}|^2 \overset{\text{sharp}}{\approx} A_p^{-2B_u}, \quad (45)$$

using the sharp-filter approximation for $|P(b_p)|^2$; and

$$I_\infty = \int_{-\infty}^{\infty} |P(\beta)|^2 d\beta I_\infty = \lim_{n \rightarrow \infty} J(\beta) \Big|_{-n}^n, \quad (46)$$

with,

$$\begin{aligned} J(\beta) &= \int^{\beta} |P(\beta')|^2 d\beta' \\ &\stackrel{\text{sharp}}{\approx} \int^{\beta} \left((A_p^2 + (\beta' - b_p)^2)^{-B_u/2} \right)^2 d\beta' \\ &= \underbrace{\frac{\beta - b_p}{A_p^{2B_u}}}_{\triangleq c} {}_2F_1\left(\frac{1}{2}, B_u; \frac{3}{2}; -\left(\frac{\beta - b_p}{A_p}\right)^2\right), \end{aligned} \quad (47)$$

using the sharp-filter approximation for $|P(\beta)|^2$. This expression is in terms of the Gauss Hypergeometric Function (GHF), which - for the case of $|z| > 1$ ¹², is expressed as,

$$\begin{aligned} {}_2F_1(a, b; c; z) &= \frac{\Gamma(b-a)\Gamma(c)}{\Gamma(b)\Gamma(c-a)} (-z^{-1})^a {}_2F_1(a, a-c+1; a-b+1; z^{-1}) \\ &+ \frac{\Gamma(a-b)\Gamma(c)}{\Gamma(a)\Gamma(c-b)} (-z^{-1})^b {}_2F_1(b, b-c+1; -a+b+1; z^{-1}). \end{aligned} \quad (48)$$

To use equation 48 for equation 47 of the ERB, we define z and y as

$$z = -y = -\left(\frac{\beta - b_p}{A_p}\right)^2, \quad (49)$$

with $|\beta| \rightarrow \infty \implies z \rightarrow -\infty$, and with $a = \frac{1}{2}, b = B_u, c = \frac{3}{2}$, and $\Gamma(1/2) = \sqrt{\pi}, \Gamma(3/2) = \sqrt{\pi}/2, \Gamma(1) = 1$.

As a result, we have,

$$\begin{aligned} {}_2F_1\left(\frac{1}{2}, B_u; \frac{3}{2}; -y\right) &= \frac{\Gamma(B_u - \frac{1}{2})\sqrt{\pi}}{\Gamma(B_u)1} y^{-\frac{1}{2}} {}_2F_1\left(\frac{1}{2}, 0; \frac{3}{2} - B_u; -y^{-1}\right) \\ &+ \frac{\Gamma(\frac{1}{2} - B_u)\sqrt{\pi}}{\sqrt{\pi}\Gamma(\frac{3}{2} - B_u)} y^{-B_u} {}_2F_1\left(B_u, B_u - \frac{1}{2}; B_u + \frac{1}{2}; -y^{-1}\right) \end{aligned} \quad (50)$$

The first GHF in the above expression is simply 1 due to the zero argument. We expand the second term using the formula for GHF for $|z| < 1$,

$${}_2F_1(a, b; c; z) = 1 + \frac{ab}{c}z + O(z^2) \quad (51)$$

and obtain,

$$\begin{aligned} {}_2F_1\left(\frac{1}{2}, B_u; \frac{3}{2}; -y\right) &= a_1 y^{-\frac{1}{2}} \\ &+ a_2 y^{-B_u} \left(1 + B_u \frac{B_u - \frac{1}{2}}{B_u + \frac{1}{2}} (-y^{-1}) + O(y^{-2})\right), \end{aligned} \quad (52)$$

with,

$$\begin{aligned} a_1 &= \frac{\sqrt{\pi} \Gamma(B_u - \frac{1}{2})}{2 \Gamma(B_u)} \\ a_2 &= \frac{1}{2} \frac{\Gamma(\frac{1}{2} - B_u)}{\Gamma(\frac{3}{2} - B_u)}. \end{aligned} \quad (53)$$

Substituting the above expansion for ${}_2F_1(\frac{1}{2}, B_u; \frac{3}{2}; -y)$ for large y into equation 47 for $J(\beta)$, we get,

¹²which is the relevant form of the GHF in our case taking $\beta \rightarrow \infty, -\infty$

$$\begin{aligned} J(\beta) &= \frac{\beta - b_p}{A_p^{2B_u}} a_1 y^{-\frac{1}{2}} \\ &+ a_2 y^{-B_u} \left(1 + B_u \frac{B_u - \frac{1}{2}}{B_u + \frac{1}{2}} (-y^{-1}) + O(y^{-2})\right). \end{aligned} \quad (54)$$

As $|\beta| \rightarrow \infty$, because $B_u > 1$, all but the first term go to zero, leaving,

$$\begin{aligned} \lim_{|\beta| \rightarrow \infty} J(\beta) &= \frac{\beta - b_p}{A_p^{2B_u}} a_1 y^{-\frac{1}{2}} \\ &= \frac{\beta - b_p}{A_p^{2B_u}} a_1 \left(\left(\frac{\beta - b_p}{A_p}\right)^2\right)^{-\frac{1}{2}} \\ &= \frac{\beta - b_p}{A_p^{2B_u}} a_1 \frac{A_p}{|\beta - b_p|} \\ &= a_1 A_p^{1-2B_u} \frac{\beta - b_p}{|\beta - b_p|}. \end{aligned} \quad (55)$$

Therefore,

$$\lim_{\beta \rightarrow \infty} J(\beta) = a_1 A_p^{1-2B_u}, \quad (56)$$

$$\lim_{\beta \rightarrow -\infty} J(\beta) = -a_1 A_p^{1-2B_u}, \quad (57)$$

which result in,

$$I_\infty = 2a_1 A_p^{1-2B_u} = \sqrt{\pi} \frac{\Gamma(B_u - \frac{1}{2})}{\Gamma(B_u)} A_p^{1-2B_u} \quad (58)$$

and consequently (as shown in equation 22),

$$\text{ERB}_\infty = \sqrt{\pi} \frac{\Gamma(B_u - \frac{1}{2})}{\Gamma(B_u)} A_p, \quad (59)$$

and its associated quality factor,

$$Q_{erb} = \frac{b_p}{\sqrt{\pi} A_p} \frac{\Gamma(B_u)}{\Gamma(B_u - \frac{1}{2})}. \quad (60)$$

While this representation is far superior to that using GHF as in equation 47, it may be further simplified to avoid using Γ functions.

To do so, we note the following: let us consider the combination of filter characteristics, $\log(\text{ERB} \times N)$ (computed using equations 59 and 18) which is purely a function of B_u . We find that this compound characteristic is very well approximated by a line $B_u > \frac{3}{2}$ ¹³. The best line for fitting to the above expression is,

$$\log\left(\frac{Q_{erb}}{\beta_{peak} N}\right) = b - a \log(B_u), \quad \text{with } b = 1.02, a = 0.418. \quad (61)$$

Substituting our expressions for N (equation 18) and β_{peak} (equation 17 in equation 61, we arrive at,

$$\log(Q_{erb}) = b + \log\left(\frac{b_p}{2\pi A_p}\right) + (1-a) \log(B_u), \quad (62)$$

which we take the exponential of in order to arrive at our simplified expression for ERB and Q_{erb} (equation 23 or table II).

¹³It is important to note that we do not use the line approximation for the case of $B_u = 1$ (second order systems). However, that is the single candidate integer point we are interested in below $\frac{3}{2}$. As a result, when expressing the filter characteristics in terms of the filter constants (to derive the inverse), we may use a piece-wise expression - with the value = $\frac{\Gamma(B_u)}{\Gamma(B_u + \frac{1}{2})} = \frac{2}{\sqrt{\pi}}$ for $B_u = 1$ and the approximation derived above otherwise (for $B_u \geq 2$). As a side note, we point out that the n dB bandwidths derived in the main text do not require this different treatment of $B_u = 1$.

REFERENCES

- [1] W.-S. Lu and T. Hinamoto, "Design of least-squares and minimax composite filters," *IEEE Transactions on Circuits and Systems I: Regular Papers*, vol. 65, no. 3, pp. 982–991, 2017.
- [2] M. F. S. Gálvez, S. J. Elliott, and J. Cheer, "Time domain optimization of filters used in a loudspeaker array for personal audio," *IEEE/ACM Transactions on Audio, Speech, and Language Processing*, vol. 23, no. 11, pp. 1869–1878, 2015.
- [3] D. N. Milic, E. Avignon-Meseldzija, J. A. Anastasov, H. Meliani, and A. Benlarbi-Delai, "A robust algorithm for the design of wideband positive-slope linear group delay filters," *IEEE Transactions on Circuits and Systems I: Regular Papers*, vol. 69, no. 10, pp. 4258–4271, 2022.
- [4] S. Nordebo, I. Claesson, and M. Dahl, "On the use of remes multiple exchange algorithm for linear-phase fir filters with general specifications," *IEEE Transactions on Education*, vol. 43, no. 4, pp. 460–463, 2000.
- [5] A. S. Alkhairy, K. G. Christian, and J. S. Lim, "Design and characterization of optimal fir filters with arbitrary phase," *IEEE Transactions on Signal Processing*, vol. 41, no. 2, pp. 559–572, 1993.
- [6] A. Alkhairy, "Design of optimal iir filters with arbitrary magnitude," *IEEE Transactions on Circuits and Systems II: Analog and Digital Signal Processing*, vol. 42, no. 9, pp. 618–620, 1995.
- [7] W. Chen, M. Huang, and X. Lou, "Design of sparse fir filters with reduced effective length," *IEEE Transactions on Circuits and Systems I: Regular Papers*, vol. 66, no. 4, pp. 1496–1506, 2018.
- [8] C. Dai, W. Chen, and Y. Zhu, "Seeker optimization algorithm for digital iir filter design," *IEEE transactions on industrial electronics*, vol. 57, no. 5, pp. 1710–1718, 2009.
- [9] N. Karaboga, "Digital iir filter design using differential evolution algorithm," *EURASIP Journal on Advances in Signal Processing*, vol. 2005, pp. 1–8, 2005.
- [10] G. Pepe, L. Gabrielli, S. Squartini, L. Cattani, and C. Tripodi, "Gravitational search algorithm for iir filter-based audio equalization," in *2020 28th European Signal Processing Conference (EUSIPCO)*, pp. 496–500, IEEE, 2021.
- [11] G. Pepe, L. Gabrielli, S. Squartini, C. Tripodi, and N. Strozzi, "Deep optimization of parametric iir filters for audio equalization," *IEEE/ACM Transactions on Audio, Speech, and Language Processing*, vol. 30, pp. 1136–1149, 2022.
- [12] S. A. Alkhairy, "Rational-exponent filters with applications to generalized auditory filterbanks," *IEEE Transactions on Circuits and Systems I: Regular Papers*, submitted.
- [13] T. Jiang and J. Zheng, "Automatic phase picking from microseismic recordings using feature extraction and neural network," *IEEE Access*, vol. 8, pp. 58271–58278, 2020.
- [14] A. A. Dibazar, S. George, and T. W. Berger, "Statistical spiking model for real world pattern recognition applications," in *The 2010 International Joint Conference on Neural Networks (IJCNN)*, pp. 1–4, IEEE, 2010.
- [15] Z. K. Abdul, A. K. Al-Talabani, and D. O. Ramadan, "A hybrid temporal feature for gear fault diagnosis using the long short term memory," *IEEE Sensors Journal*, vol. 20, no. 23, pp. 14444–14452, 2020.
- [16] A. Karlos and S. J. Elliott, "Cochlea-inspired design of an acoustic rainbow sensor with a smoothly varying frequency response," *Scientific Reports*, vol. 10, no. 1, p. 10803, 2020.
- [17] W. Zhang, Y. Wu, D. Wang, Y. Wang, Y. Wang, and L. Zhang, "Underwater target feature extraction and classification based on gammatone filter and machine learning," in *2018 international conference on wavelet analysis and pattern recognition (ICWAPR)*, pp. 42–47, IEEE, 2018.
- [18] S. Cosentino, T. H. Falk, D. McAlpine, and T. Marquardt, "Cochlear implant filterbank design and optimization: A simulation study," *IEEE/ACM Transactions on Audio, Speech, and Language Processing*, vol. 22, no. 2, pp. 347–353, 2013.
- [19] T. Harczos, A. Chilian, and P. Husar, "Making use of auditory models for better mimicking of normal hearing processes with cochlear implants: the sam coding strategy," *IEEE transactions on biomedical circuits and systems*, vol. 7, no. 4, pp. 414–425, 2012.
- [20] G. Yang, R. F. Lyon, and E. M. Drakakis, "A 6 uw per channel analog biomimetic cochlear implant processor filterbank architecture with across channels agc," *IEEE transactions on biomedical circuits and systems*, vol. 9, no. 1, pp. 72–86, 2014.
- [21] F. Alfás, J. C. Socoró, and X. Sevillano, "A review of physical and perceptual feature extraction techniques for speech, music and environmental sounds," *Applied Sciences*, vol. 6, no. 5, p. 143, 2016.
- [22] S. Kortlang, S. D. Ewert, and T. Gerkmann, "Single channel noise reduction based on an auditory filterbank," in *2014 14th International Workshop on Acoustic Signal Enhancement (IWAENC)*, pp. 283–287, IEEE, 2014.
- [23] D. M. Agrawal, H. B. Sailor, M. H. Soni, and H. A. Patil, "Novel teo-based gammatone features for environmental sound classification," in *2017 25th European Signal Processing Conference (EUSIPCO)*, pp. 1809–1813, IEEE, 2017.
- [24] A. Badi, K. Ko, and H. Ko, "Bird sounds classification by combining pncc and robust mel-log filter bank features," *The Journal of the Acoustical Society of Korea*, vol. 38, no. 1, pp. 39–46, 2019.
- [25] M. M. Milani, M. Ramashini, and M. Krishani, "Speech signal analysis of covid-19 patients via machine learning approach," in *2021 International Conference on Decision Aid Sciences and Application (DASA)*, pp. 314–319, IEEE, 2021.
- [26] B. Alexander, G. Nallathambi, and N. Selvaraj, "Screening of heart sounds using hidden markov and gammatone filterbank models," in *2018 17th IEEE International Conference on Machine Learning and Applications (ICMLA)*, pp. 1460–1465, IEEE, 2018.
- [27] Z. Neili and K. Sundaraj, "A comparative study of the spectrogram, scalogram, melspectrogram and gammatonegram time-frequency representations for the classification of lung sounds using the icbhi database based on cnns," *Biomedical Engineering/Biomedizinische Technik*, vol. 67, no. 5, pp. 367–390, 2022.
- [28] C. Zhou, Y. Wu, Z. Fan, X. Zhang, D. Wu, and Z. Tao, "Gammatone spectral latitude features extraction for pathological voice detection and classification," *Applied Acoustics*, vol. 185, p. 108417, 2022.
- [29] D. A. Hague, J. R. Buck, and I. Bilik, "A deterministic compressive sensing model for bat biosonar," *The Journal of the Acoustical Society of America*, vol. 132, no. 6, pp. 4041–4052, 2012.
- [30] Z. Tu, N. Ma, and J. Barker, "Dhasp: Differentiable hearing aid speech processing," in *ICASSP 2021-2021 IEEE International Conference on Acoustics, Speech and Signal Processing (ICASSP)*, pp. 296–300, IEEE, 2021.
- [31] T. Zhang, F. Mustiere, and C. Micheyil, "Intelligent hearing aids: The next revolution," in *2016 38th Annual International Conference of the IEEE Engineering in Medicine and Biology Society (EMBC)*, pp. 72–76, IEEE, 2016.
- [32] N. Jankovic, V. Crnojevic-Bengin, P. Meyer, and J.-S. Hong, "Design methods of multi-band filters," *Advances in Multi-Band Microstrip Filters*, pp. 5–66, 2015.
- [33] W. Feng, C. Wang, X. Chen, Y. Shi, M. Jiang, and D. Wang, "Filter realization of the time-domain average denoising method for a mechanical signal," *Shock and Vibration*, vol. 2021, pp. 1–13, 2021.
- [34] S. A. Alkhairy and C. A. Shera, "An analytic physically motivated model of the mammalian cochlea," *The Journal of the Acoustical Society of America*, vol. 145, no. 1, pp. 45–60, 2019.
- [35] C. J. Galbraith, R. D. White, L. Cheng, K. Grosh, and G. M. Rebeiz, "Cochlea-based rf channelizing filters," *IEEE Transactions on Circuits and Systems I: Regular Papers*, vol. 55, no. 4, pp. 969–979, 2008.
- [36] A. G. Katsiamis, E. M. Drakakis, and R. F. Lyon, "Practical gammatone-like filters for auditory processing," *EURASIP Journal on Audio, Speech, and Music Processing*, vol. 2007, pp. 1–15, 2007.
- [37] K. K. Charaziak and A. Altoè, "Estimating cochlear impulse responses using frequency sweeps," *The Journal of the Acoustical Society of America*, vol. 153, no. 4, pp. 2251–2251, 2023.
- [38] S. A. Alkhairy, *An analytic model of the cochlea and functional interpretations*. PhD thesis, Massachusetts Institute of Technology, 2017.
- [39] S. A. Alkhairy, "Cochlear wave propagation and dynamics in the human base and apex: Model-based estimates from noninvasive measurements," in *Nonlinearity and Hearing: Advances in theory and experiment: Proceedings of the 14th International Mechanics of Hearing Workshop*, AIP Publishing, 2022.
- [40] C. A. Shera and J. J. Guinan Jr, "Stimulus-frequency-emission group delay: A test of coherent reflection filtering and a window on cochlear tuning," *The Journal of the Acoustical Society of America*, vol. 113, no. 5, pp. 2762–2772, 2003.